The nature of surface deposits following valeric acid interactions with Al_2O_3-supported Alkaline Earth Oxide catalysts: Towards cellulosic biofuels.

James A Sullivan*, Nichola Walsh and Linda Sherry,

UCD School of Chemistry and Chemical Biology,
Belfield,
Dublin 4,
Ireland.

e-mail: james.sullivan@ucd.ie, linda.sherry@ucd.ie , nichola.walsh@ucd.ie

Abstract

Two Al_2O_3-supported alkaline earth metal oxide catalysts (MgO and BaO) were contacted with valeric acid at 250 °C. Each formed amounts of 5-nonanone (BaO more than MgO). A significant deposition of hydrocarbonaceous material onto the catalyst surface is noted. This adsorbed material is characterised using TGA and FTIR and relates to a carboxylate species.

Keywords: Cellulosic biodiesel, basic catalysts, catalyst characterisation.

Introduction.

The increasing economic and social costs associated with the use of petroleum derived fuels have led to significant research interest in the development of replacement sustainable supplies of liquid fuel [1].

The use of renewable biomass to produce liquid fuels would ameliorate these problems [2] and this has led to the development of several industrial processes for

the production of bio-ethanol *e.g.* [3] and biodiesel *e.g.* [4] fuels where the biomass substrates are maize and vegetable oils respectively. The use of these fuels suffers from several problems which include the diversion of a food resource to a cash crop, a significant amount of plant matter wastage and the overall carbon balance of production in several cases being negative [5].

Recently, work has begun on the production of bioethanol and biodiesel (as well as a range of other commodity chemicals) from cellulosic feedstocks [6 - 10]. Cellulose is a polymer of glucose monomeric units linked together using α l – 4 linkages. It forms a large part of the structure of woody and grassy plants. Crops with high levels of cellulose can be produced on non-arable land, with little fertilizer use and waste is minimal and there has been much recent work in using this feedstock to generate usable fuels [11-14].

Hydrolysis of cellulose using the “Biofine” (and related) process generates (in approximately 50% yield) an equimolar mixture of levulinic acid (LA) and formic acid. Hydrogenation of levulinic acid using two equivalents of H_2 generates (*via* γ valerolactone (gVL)) valeric acid (VA) [15, 16] (see figure 1(a)). There has been significant recent interest in the use of valeric acid for the production of biodiesel [17 – 21] and, in particular the use of the ketonic decarboxylation reaction to form 5-nonanone (see figure 1(b)) [22, 23].

The reactions of a wide range of carboxylic acids over an equally wide range of oxide surfaces has attracted significant attention both from fundamental and applied perspectives *e.g.* [24-27]. In general, carboxylate and enolate species are discussed as intermediates over a range of reducible, refractory and rare earth oxides. Very

few of these reports have looked at the use of supported alkaline earth oxide materials as catalysts.

Herein we study the interactions between VA and two model basic catalysts (Al_2O_3 supported MgO and BaO). TGA and FTIR are used to monitor these interactions. TGA of the catalyst post reaction allows us to quantify the extent of adsorption (through analysis of the total mass loss) and also to say something about the nature of the adsorbed species (through analysis of their temperature of combustion).

Experimental.

Catalyst preparation: 10%BaO/γAl_2O_3 and 10%MgO/γAl_2O_3 were prepared *via* incipient wetness impregnation. The support (BET S.A. ~195 m^2 g^{-1}, pore volume ~1.7 mL g^{-1}) was crushed and sieved to form particles in the 800 μm range.

The catalysts were loaded with 10 % metal oxide using solutions of $Ba(CH_3CO_2)_2$ and $Mg(CH_3CO_2)_2$ precursors. They were dried at 80 °C for 1h and calcined at 500 °C for 4 h to oxidise the acetates to their respective oxides.

When required, valeric acid was added to these fresh materials *via* H_2O suspension (250 μmol g^{-1} diluted to the material's pore volume). This loading of VA is significantly lower than that used during the catalytic reaction.

Reactivity studies: Reactions were performed in a plug flow reactor (PFR). 0.1 g aliquots of the catalysts (which had been pre-treated in air at 500 °C before being cooled to 250 °C) were held between two plugs of quartz wool in a quartz microreactor. Liquid phase valeric acid (16.5 μL min^{-1}) was fed from a calibrated syringe driver (Hamilton) into heated (190 °C) tubing where it vaporised. The gas

was carried over the catalyst by an N_2 carrier gas flow (60 mL min^{-1}). The reactions were continued for 30 minutes. These conditions were chosen as a set where some measurable conversion was attained.

The exit gases of the reactor were collected in a vessel cooled in an N_2-acetone slush bath to condense the liquid phase products. Following reaction, the volume of the collected product mixture was measured and the solution was analysed by GC (Shimadzu GC-14B) with a DB-5 column (Agilent) and a flame ionisation detector (FID). Dodecane was used as a standard during these measurements.

Thermogravimetric Analysis: Samples were suspended on the platinum pan of a Q500 TGA (TA Instruments) in a flow of (90 mL min^{-1}) air and subject to a temperature ramp of 10 °C min^{-1} from room temperature to 800 °C. Any weight changes monitored are displayed as derivative weight change profiles.

FTIR characterisation: Difference DRIFTs and *in-situ* DRIFTs experiments were carried out using a Vertex 70 (Bruker) spectrometer, equipped with an MCT detector, a diffuse reflectance accessory (Praying Mantis – Harrick) and a high temperature catalytic reaction chamber (HVC-DRP – Harrick). The samples were placed in the *in-situ* cell which allowed control of the temperature and gaseous atmosphere). All spectra were recorded in transmittance mode between 600 and 4000 cm^{-1} with a resolution of 2 cm^{-1}. All materials were ground using standard pestle and mortar prior to collection of the spectra. Background spectra were recorded using a fresh catalytic sample.

Results and Discussion

Reactivity studies: Both catalysts converted a certain amount of valeric acid to 5-nonanone (following exposure to ~ 4 mmol valeric acid) within the plug flow reactor when the catalyst was held at 250 °C. These conversions were extremely low and a carbon balance was not achieved. The BaO catalyst was more active than the MgO analogue by approximately an order of magnitude (2 μmol of 5-nonanone were formed over the MgO catalyst and 26 μmol over the BaO catalyst). Interestingly, no side products were observed by GC in the collected liquid in either case with only valeric acid and 5-nonanone being detected. Significant amounts of material were deposited onto the catalyst during the reaction as evidenced both from the discolouration of the catalyst and the propensity of the deposits to form a tar which subsequently blocked the reactor. The latter problem was avoided by the use of an inert diluent (α Al_2O_3).The principal results reported here relate to the characterisation of this deposited material.

TGA characterisation: TGA profiles for both catalysts prior to and following reaction are shown in Figure 2. Prior to reaction (❍) the profiles show dehydration of both the supported MgO and BaO catalysts at low temperatures (~100 °C) as well as a small mass loss at higher temperatures relating to surface carbonate decomposition from the MgO/Al_2O_3 catalyst at T> 600 °C. In both cases, for the fresh catalyst approximately 6% of the mass of the catalyst was lost during these experiments due to the loss of adsorbed CO_2 and H_2O as well as de-hydroxylation at higher temperatures.

The TGA profiles from the two catalysts following exposure to valeric acid under reaction conditions are also shown in figure 3 (□). There are several extra features in these profiles showing the oxidation of the material deposited onto the surface

during the reaction. Approximately 21% and 18% mass loss was noted during TGA of the BaO and MgO catalysts respectively, *i.e.* more material had been deposited onto the supported BaO catalyst during the reaction.

In both cases the initial weight loss below 100 °C from the used materials is likely to be attributed to H_2O desorption (as was the case with the fresh catalysts). In the case of 10%BaO/Al_2O_3, there are three other weight loss events (centred at 170, 250 and 340 °C) which are not present in the DTGA of the fresh material. However, the 10%MgO/Al_2O_3 catalyst only appears to have two such oxidation / decomposition / desorption events (centred at 180 and 340 °C), with an additional high temperature shoulder centred at 465 °C off the major DTG peak. It is reasonable to assume that these peaks relate to the combustion of either un-reacted valeric acid, some reaction intermediate or adsorbed product.

With the aim of clarifying whether un-reacted VA contributed to this peak we carried out an experiment where valeric acid was dosed onto the catalysts at room temperature and the un-reacted valeric acid characterised using TGA. Figure 3 shows these profiles from the supported MgO (△) and BaO (✧) catalysts.

From both materials, DTG peaks are seen as a shoulder (centred ~ 180 °C) with a major peak at 330 °C and a further shoulder centred at 475 °C – with the latter being much more apparent from the MgO catalyst. These differences between the DTG profiles from the BaO and the MgO containing materials suggest that adsorbed VA is removed (either through oxidation, decomposition or desorption) from these materials in slightly different manners.

Regarding the substantive issue (*i.e.* attempts to assign the different reaction events seen in the TGA of the post-reaction materials), these profiles can be compared to

those from the post-reaction materials. In the case of the 10%BaO/Al_2O_3 (the more active material) the DTGA profiles from the post-reaction material and the fresh sample dosed with valeric acid match rather well, *i.e.* there are peaks at ~ 180 °C and 325 °C in both cases. This suggests that there is un-reacted valeric acid (or some species with the same oxidation characteristics as valeric acid) adsorbed onto the surface of the material after the reaction at 250 °C in the PFR.

In the case of the DTGA from the sample following reaction however, there is a further peak at ~ 240 °C which is absent in the profile from the sample dosed with VA at room temperature (see figure 3(b)). The mass loss from the catalyst seen at 240 °C must relate to the combustion of another species formed on the surface during reaction. This may be some reaction intermediate, some adsorbed 5-nonanone product or a side product of the ketonic decarboxylation reaction.

A further difference between the profiles of the post-reaction material and the material dosed with VA at room temperature is the absence of the high temperature shoulder present in the latter profiles (centred at 475 °C) but absent in the DTGA profile of the 10%BaO/Al_2O_3 catalyst following reaction.

Comparing the profiles from the post-reaction 10%MgO/Al_2O_3 catalyst with those from fresh samples of the same material dosed with valeric acid at room temperature, it is clear that all of the peaks created from the valeric acid oxidation / decomposition / desorption are present in the profile of the post-reaction material (including the shoulder between 400 – 550 °C). This suggests the presence of un-reacted VA (or some species with the same combustion properties of this material) on the 10%MgO/Al_2O_3 catalyst, which adsorbed during reaction.

FTIR Characterisation: The nature of the adsorbate has also been characterised using difference FTIR spectroscopy. A difference FTIR spectrum of an aliquot of the 10%MgO/Al_2O_3 following the reaction was recorded using a sample of fresh 10%MgO/Al_2O_3 material as the spectral background. The spectrum was recorded in transmittance mode, and in the plots below peaks showing decreased transmittance are related to vibrations which arise from adsorbed species deposited on the catalyst during reaction. Any peaks with > 100% transmittance are a result of functional groups which were initially present on the fresh material but which have been modified or removed as following interaction between the catalyst and VA at 250 °C.

This difference spectrum can be seen in figure 4 along with a spectrum of an equivalent sample which had been dosed with VA at room temperature (as in the TGA studies above).

If we firstly focus on the sharp positive peaks (which relate to species removed from the catalyst upon interaction with VA) centred at 3700 cm^{-1} in both spectra we can assign these to decreases in surface hydroxyl concentration. The broad band in this region, centred at 3500 cm^{-1} which is also found in both spectra, represents a displacement of H_2O from the surface. This supports an adsorption mechanism where the OH group on VA is deprotonated by the surface hydroxyl of the catalyst. This is probably the initial step in ketonic decarboxylation.

Also evident are bands in the regions between 2800–3000 cm^{-1} and 1350–1500 cm^{-1}. These can be assigned to C-H stretches and bends respectively from the adsorbed valeric acid, 5-nonanone product or some intermediate species. This confirms the TGA results which showed adsorbed oxidisable species remained on the surface following reaction.

A significant difference between these spectra is the presence of a broad peak centred at 2568 cm^{-1} in the case of the material dosed with VA at room temperature. According to Pavia *et al*. [28] this is the region in which carboxylic acid OH vibrations occur. The absence of this peak in the spectrum of the post-reaction material suggests that the OH group of VA is no longer present, and has been consumed or modified by the reaction. In the case of the room temperature adsorption, a %T > 100 at 3700 cm^{-1} indicates removal / modification of the catalyst's surface hydroxyls (as above in the case of the post reaction material). However, the presence of a band at 2568 cm^{-1} suggests that a portion of the valeric acid on the surface remains unreacted.

A further difference is seen in the carbonyl region of both spectra. In the case of the material dosed with VA at room temperature, a strong carbonyl peak appears at 1727 cm^{-1} (in unbound valeric acid this peak appears at 1711 cm^{-1}). This peak's intensity has been dramatically decreased and its position has shifted in the spectrum of the post-reaction catalyst (1700 cm^{-1}) confirming that the carboxylic acid functional group has been some way altered during the reaction at 250 °C.

In the case of the post-reaction material there also is a strong peak observed at 1575 cm^{-1} which is only weakly present in the spectrum of the material dosed with VA at room temperature. Absorbance at such a low energy is suggestive of a carboxylate species [29]. This provides evidence for the formation of a valerate species on the surface of the catalyst after reaction at 250 °C following VA deprotonation.

A far less intense peak is seen at this position from the sample that had been exposed to VA at room temperature (suggesting a small amount of deprotonation had taken place at low temperature).

These spectra suggest that there is a small amount of reaction (evidenced from the weakly present carboxylate peak) and significant amounts of un-reacted valeric acid (represented by the carboxylic acid CO and OH peaks) remaining on the surface at room temperature. For species adsorbed on the post-reaction material there appears to be very little un-reacted valeric acid (as demonstrated by the relatively small peak at 1700 cm^{-1}), but a high concentration of carboxylates.

Temperature effects on FTIR spectra of adsorbed Valeric acid: To further study the conversion of VA on the surfaces of these catalysts, a suspension of VA was dosed to a pre-hydroxylated catalyst (where hydroxylation was carried out by repeatedly wetting the catalysts at room temperature and drying at 120 °C for 30 minutes). The samples were then dried at 120 °C for 30 minutes and cooled. Subsequently they were heated to different temperatures (120 °C, 150 °C and 300 °C) in an inert atmosphere, for 1 minute, cooled to room temperature and their FTIR spectra were recorded. Figure 5 shows the spectra recorded after samples were heated to 120 °C and 300 °C.

As well as showing the expected hydrocarbonaceous C-H stretches and bends (see above), a carboxylate stretch (at ~1570 cm^{-1}) is seen on both catalysts. This change in the carbonyl stretch (1711 cm^{-1} in pure VA and 1727 cm^{-1} in adsorbed un-reacted VA) shows that exposure of the adsorbed species to a temperature of 120 °C for ~30 minutes (during the drying process) is sufficient to convert the adsorbed VA into a carboxylate species. These effects have also previously been seen for other carboxylic acids over different oxide catalysts [24, 25].

Treatment of the adsorbed material on BaO catalyst to 300 °C resulted in the generation of a blue shifted shoulder in the carbonyl / carboxylate region of the spectrum. This change was not noted in the case of the less active MgO material.

The increased transmittances of the negative hydroxyl peak (~3650 cm^{-1}) seen following treatment at higher temperatures over both catalysts suggest de-hydroxylation of the surfaces. In the case of MgO there is also a change in position of this negative peak under these conditions. This has been noted previously and ascribed to the removal of $Mg(OH)_2$ from the surface at higher temperatures [30].

The sharp negative peaks associated with the removal of the surface hydroxyl species following interaction with VA (figure 4) are not as noticeable in these spectra but it should be recalled that these samples would have had a significantly higher concentration of surface hydroxyls making the difference spectra less sensitive to such small changes.

In any case, these results show that the de-protonation of VA over these materials progresses at relatively low temperatures but that the de-protonated residue is relatively stable over both catalysts (albeit being slightly more reactive on the BaO catalyst). Future work will study whether this deposit is a poison for the catalytic reaction.

Conclusions.

Supported MgO and BaO can, to limited extents, catalyse ketonic decarboxylation of VA at 250 °C. BaO is more active than MgO. In both cases, a hydrocarbonaceous residue remains on the catalyst. FTIR has shown that this is a relatively stable carboxylate formed following deprotonation of VA on surface OH. Reaction happens

at low temperatures of 120 °C (but not extensively at room temperature). FTIR has also shown the conversion of carboxylate over BaO (but not over MgO) following brief treatments to 300 °C.

TGA has shown that the adsorbed material has similar combustion characteristics as adsorbed VA in the case of MgO but another adsorbed species is present on the post-reaction BaO catalysts. This may relate to the converted carboxylate species noted above.

Acknowledgements: The UCD SCCB is acknowledged for providing funding to LS.

References

1. Chemicals & materials from renewable resources. J.J.Bozell, ACS, Washington 2001.

2. J.N. Chheda, G.W. Huber and J. A. Dumesic, Angew. Chem., Int. Ed., 2007, 46, 7164-7183.

3. A. Demirbas, Progress in Energy & Combustion Science, 33, 1, 1-18 2007.

4. L.C. Meher, D.V. Sagar and S.N. Naik, Renewable & Sustainable Energy Reviews, 10, 3, 248-268, 2006.

5. P. J. Crutzen, A. R. Mosier, K. A. Smith, and W. Winiwarter. Atmos. Chem. Phys. Discuss., 7, 11191-11205, (2007)

6. N. Mosier, C. Wyman, B. Dale, R. Elander, Y.Y. Lee, M. Holtzapple, M. Ladisch, Bioresource Technology, 96, 6, 673-686, 2005.

7. A. Limayem, S.C. Ricke, Progress in Energy & Combustion Science, 38, 4, 449-467, 2012

8. S.Y. Lee, M.A. Hubbe, S. Saka, Shiro, Bioresources,1, 1, 150-171, 2006.

9. D.J Hayes, M.H.B Hayes, Biofules, Bioproducts and Biorefining, 3, 5, 500-520, 2009.

10. R. Kumar, S. Singh, V. Om, Journal of Industrial Microbiology and Biotechnology, 35, 5, 377-391, 2008.

11. D. J. Hayes, Catal. Today, (2009), 145, 138–151.

12. P. Anbarasan, Z.C. Baer, S. Sreekumar, E. Gross, J.B. Binder, H.W. Blanch, D.S. Clark, F.D. Toste, Nature, 2012, 491, 235-239

13. P. Nilges, T.R. dos Santos, F. Harnisch, U. Schroder, Energy & Environmental Science, 2012, 5, 5231-5235

14. R.S. Assary, L.J. Broadbelt, Computational and Theoretical Chemistry, 2011, 978, 160-165.

15. S. W. Fitzpatrick, Manufacture of furfural and levulinic acid by acid degradation of lignocellulose, World patent 8 910 362 to Biofine Incorporated, 1990;

16. R. Weingarten, W.C. Conner, G.W. Huber, Energy & Environmental Science, 5, 6, 7559-7574, (2012).

17. J.Q.Bond, D.Wang, D.M.Alonso, J.A.Dumesic, J.Catal., 281, 2, 290-299, 2011

18. X. Hu, C-Z. Li, Green Chemistry, 13, 7, 1676-1679, (2011)

19. G. Centi, P. Lanzafame, S. Perathoner, Catalysis Today, 167, 1, 14-30, (2011)

20. S. Van De Vyver, J. Geboers, P.A. Jacobs, B.F. ChemCatChem, 3, 1, 82-94, (2011)

21. A. Corma, M. Renz, C. Schaverien, ChemSusChem, 2008, 1, 739 – 741.

22. R. Palkovits. Angwandte Chemie-International Ed., 49, 26, 4336-4338, 2010

23. J.P. Lange, R. Proce, P.M. Ayoub, J. Louis, L.Petrus, L.Clarke, H.Gosselink, Angewandte Chemie, International Edition, 49, 4479 – 4483, 2010,.

24. L. Chen, Y. Zhu, H. Zheng, C. Zhang, B. Zhang, Y. Li, Journal of Molecular Catalysis A: Chemical, 351, 217-227, 2011.

25. Y. Yamada, M. Segawa, F. Sato, T. Kojima, Takashi, S. Sato, Journal of Molecular Catalysis A: Chemical, 246, 1-2, 79-86, 2011

26. M. Renz, Eur. J. Org. Chem., 979-988, 2005.

27. J.C. Serrano-Ruiz, D.Wang and J.A. Dumesic, Green Chemistry, 12, 574 – 577, 2010.

28. L. Pavia, V. Kriz, Introduction to Spectroscopy, 4th Ed., Brooks Cole, 2008.

29. J. Coates, Encyclopedia of Analytical Chem., John Wiley & Sons, Ltd, 2006.

30. A. Botha and C. Strydom, J. Thermal Analysis & Calorimetry, 71 (2003) 987.

Figure 1

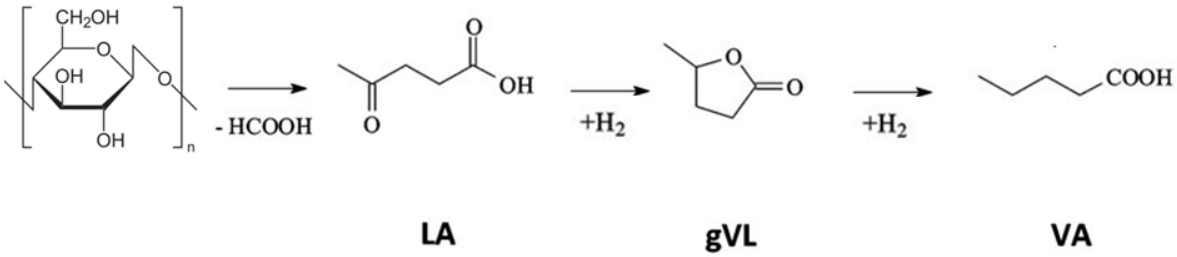

LA gVL VA

(a)

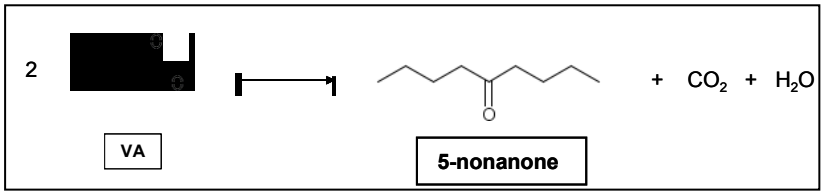

(b)

Figure 1 (a): the conversion of cellulose to Levulinic Acid (LA) *via* the "Biofine" process and selective hydrogenation to form γ Valerolactone (gVL) and Valeric Acid (VA) (b): the conversion of valeric acid to 5-nonanone *via* ketonic decarboxylation

Figure 2

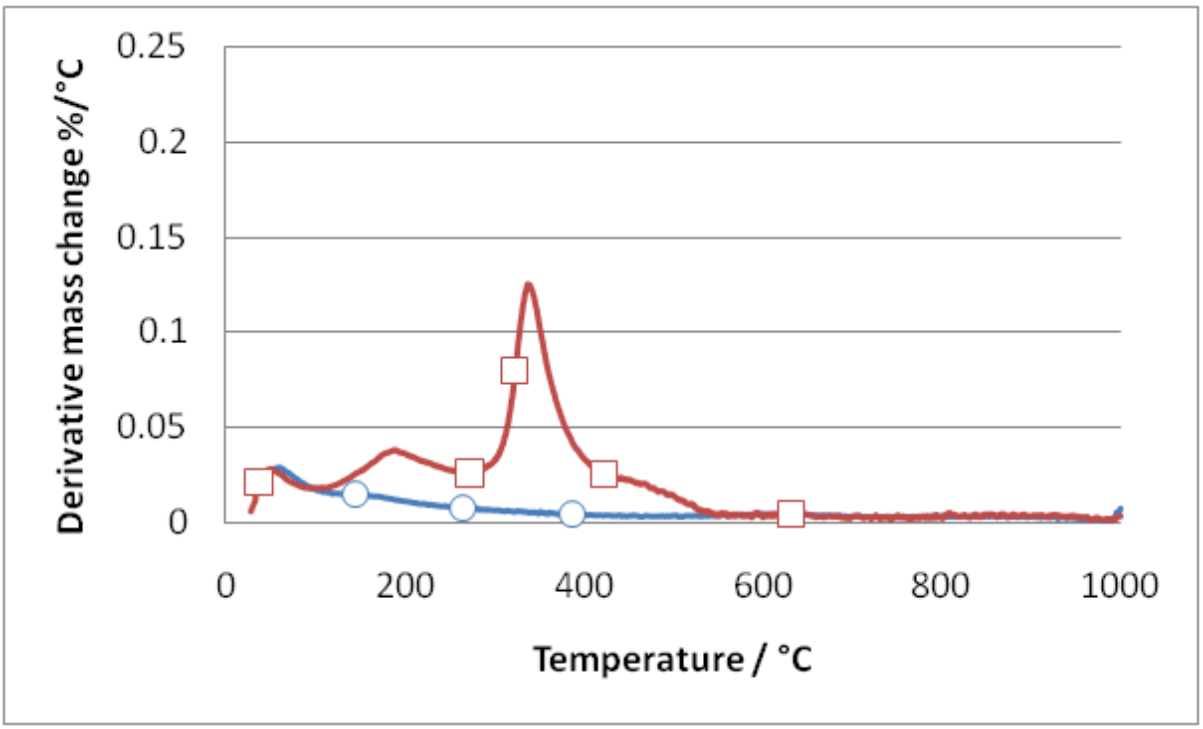

(a)

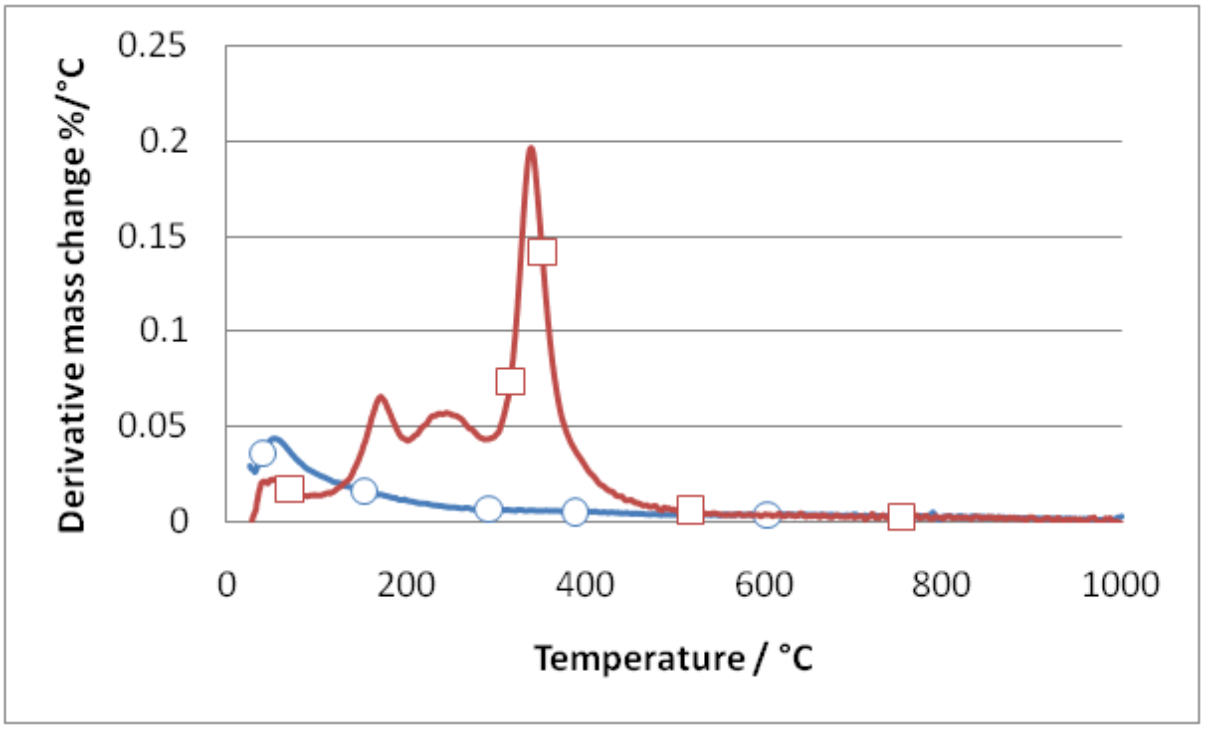

(b)

Figure 2 DTGA profiles of fresh catalysts (❍) and catalysts post-ketonic decarboxylation reaction at 250 °C (◘) (a) MgO/Al_2O_3 and (b) BaO/Al_2O_3.

Figure 3

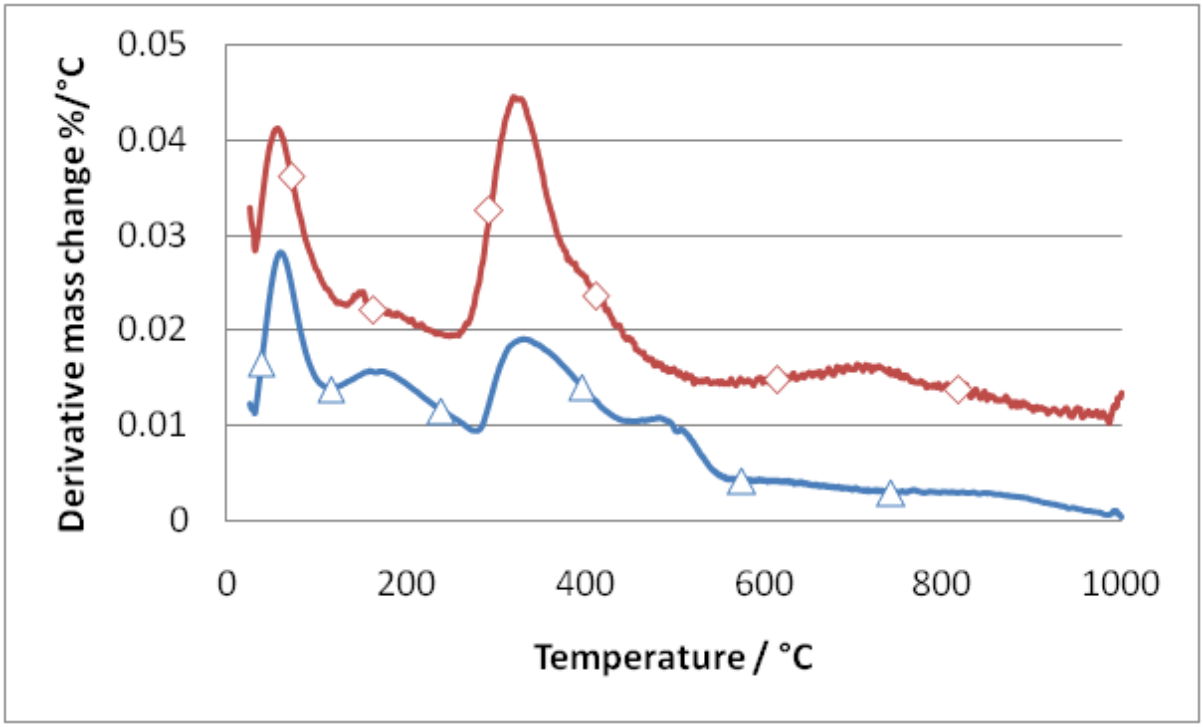

Figure 3: DTG profiles for fresh catalyst MgO/Al_2O_3, (△) and BaO/Al_2O_3 (✧) dosed with an aqueous valeric acid suspension.

Figure 4

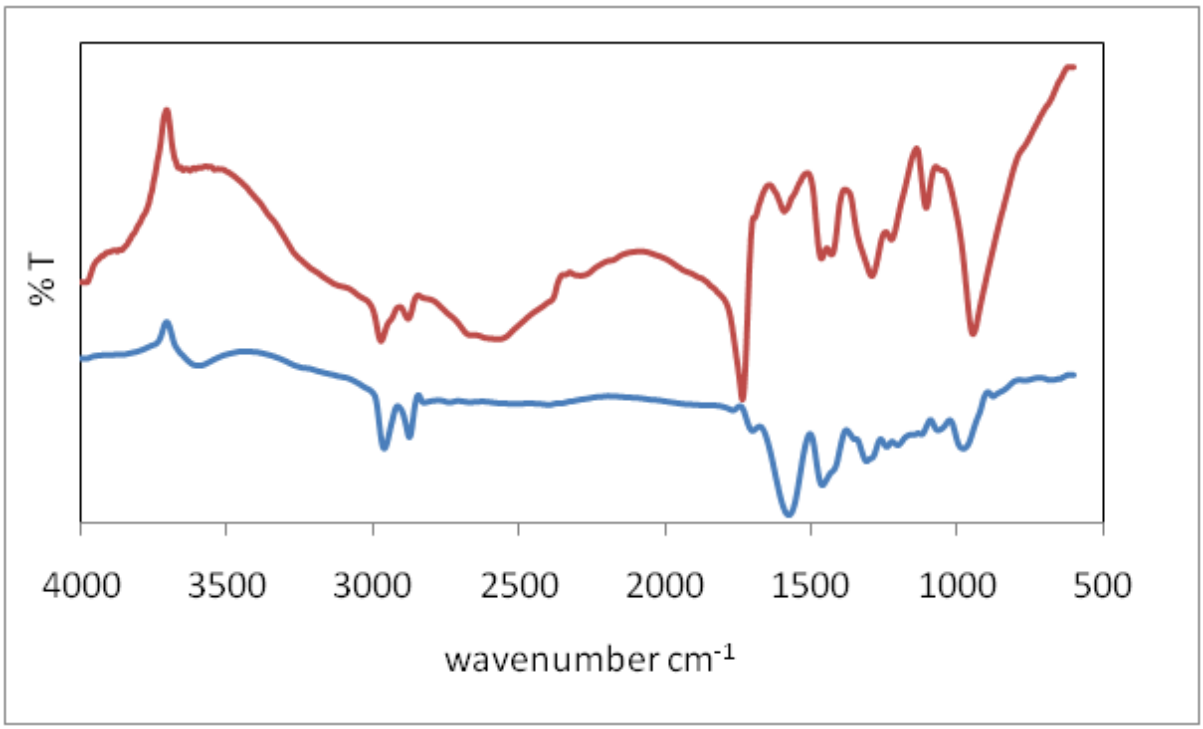

Figure 4: Difference FTIR spectra of 10%MgO/γAl_2O_3 with VA adsorbed at room temperature (upper profile) and post-reaction 10%MgO/Al_2O_3 (lower plot) (both spectra were collected using fresh 10%MgO/Al_2O_3 to record the spectral background).

Figure 5

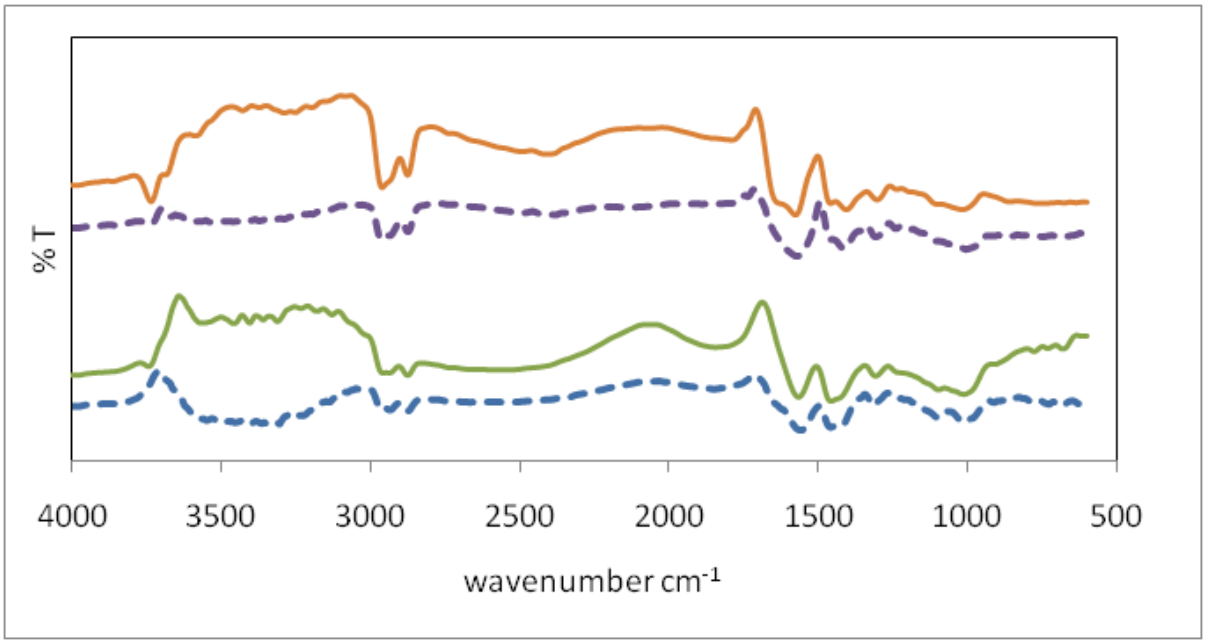

Figure 5: showing the FTIR spectra of valeric acid adsorbed on MgO (lower profiles) and BaO (upper profiles) and heated to 120 °C (dashed line) and 300 °C (full line).